Experimental and Theoretical Analysis of Argon Plasma-Enhanced Quantum-Well Intermixing

H. S. Djie, *Student Member, IEEE*, T. Mei, *Member, IEEE*, J. Arokiaraj, C. Sookdhis, S. F. Yu, *Senior Member, IEEE*, L. K. Ang, *Associate Member, IEEE*, and X. H. Tang

***Abstract*—Plasma-enhanced quantum-well intermixing (QWI) has been developed for tuning the bandgap of InGaAs–InP material using an inductively coupled plasma system. The application of inductively coupled plasma enhances the interdiffusion of point defects resulting in a higher degree of intermixing. Based on a semi-empirical model of QW interdiffusion, the bandgap blue-shift with respect to the plasma exposure time and inductively coupled plasma energy has been analyzed. The theoretical results appear to be in good agreement with the experimental data of the intermixed samples. The model serves as a good simulation tool to explain the intermixing mechanism and further to optimize the intermixing process for the fabrication of the photonic integrated circuits.**

***Index Terms*—Inductively coupled plasma, photonic integrated circuits, quantum well, quantum-well intermixing (QWI).**

I. Introduction

THERE has been a strong motivation in developing an effective quantum-well intermixing (QWI) technology to tune the quantum well (QW) properties at the postgrowth level for optoelectronic and photonic integrated circuit (PIC) applications. The monolithic InP-based ternary or quaternary PICs play an important role in optical fiber telecommunications as their operation wavelengths can match the very low loss and dispersion windows at 1.3 and 1.55 μm. The ability to modify the bandgap energy across a single substrate is a key requirement for monolithic integration of multiple photonic devices. The specifications of individual components such as gain, absorption, or transmission at the operation wavelength can be posttuned by modifying the bandgap across an InP-based semiconductor wafer. The QWI technique has generated considerable interest due to its simplicity and effectiveness. The emerged technology of QWI in the past decades [1], such as impurity-induced disordering (IID) [2], [3], focused ion beam (FIB) [4], impurity-free vacancy disordering (IFVD) [5], sputter silica-induced intermixing [6], and laser-induced disordering (LID) [7], has been utilized into wide application for PICs, such as the widely tunable sampled-grating distributed Bragg reflector laser (SGDBR) device [8].

The development of high-density plasma, such as the inductively coupled plasma (ICP) machine, enables the use of low-ion bombardment energy with high-ion bombardment fluxes. ICP reactors produce high-density plasmas (10^{10}–10^{12} cm^{-3}) at low gas pressure ($< 10'$ s mTorr). ICPs have been used for high-etch-rate, low-etch-damage applications and for depositing a wide variety of semiconductor materials including dielectrics and III-V semiconductors. The use of plasma-enhanced QWI is attractive since the low-energy (with hundreds of electronvolts of ion impact energy) ions generated in the plasma chamber produces no direct damage to the QW active region, thereby promising high-quality photonic devices for PICs application. Initial work has been done using H_2 plasma glow discharge in a reactive ion-etching (RIE) system on GaAs–AlGaAs structures. Up to eight cycles of H_2 plasma exposure and annealing is required to produce a maximum bandgap wavelength blue-shift of about 24 nm [9]. QWI using argon (Ar) plasma generated by an electron cyclotron resonance (ECR) etcher was reported [10], which produced a wavelength shift of 106 nm. Ar gas was used since it is a noble gas with a relatively high atomic weight to produce a high surface defect density for a high degree of intermixing. When Ar ions are introduced to the semiconductor material, they create point defects, including vacancies, interstitials, vacancy-interstitial (Frenkel) pairs, and antisite defects. The generation of the atoms on the wrong sublattice, called the antisites, is negligible during Ar plasma exposure to promote the intermixing between barriers and QWs as the annealing temperature used in a common QWI process. An increase of ion bombardment energy greatly raises the formation probability of surface defects, which causes surface damage to a semiconductor.

Recently, the plasma-enhanced QWI technique using an ICP machine has been well established for generating near surface point defects to promote intermixing in QW samples [11], [12]. This technique utilizes the generation of mobile point defects far from the active QW region as the Ar ions may knock ions off its crystal site of sample to produce either a single isolated vacancy or a group of vacancies. During the subsequent annealing, the created point defects can effectively propagate from one lattice to another lattice site in the random walk motion. The diffusion of point defects down to the active QW region, that subsequentlythat results from the atomic hopping in the presence of point defect propagation, will promote intermixing between the QWs and its barriers to form alloy semiconductors. This intermixing process results in an increase in the QW energy bandgap. In addition to the annealing process, the annealing treatment also recovers crystal damage on the sample surface induced by the QWI technique, and the intermixed device does not suffer significant optical degradation.

In this work, we have investigated the QWI effect of inductively coupled Ar plasma on InGaAs–InGaAsP QW structures generated in an ICP machine and wavelength shift using photoluminescence (PL) spectroscopy. The plasma property in the

Manuscript received June 6, 2003; September 23, 2003.

The authors are with the Photonics Research Centre, School of Electrical and Electronic Engineering, Nanyang Technological University, Singapore 639798 (e-mail: hery@pmail.ntu.edu.sg).

Digital Object Identifier 10.1109/JQE.2003.821542

0018-9197/04$20.00 © 2004 IEEE

ICP chamber is calculated to provide an estimation of ion dose and sheath voltage in an ICP machine. A plasma-induced defects model is proposed to understand qualitatively the created damage profiles after plasma exposure. A semi-empirical model based on the plasma-enhanced QWI technique is developed to study the effect of inductively coupled plasma application with respect to different exposure times through the interdiffusion coefficient enhancement of point defect propagation during the annealing step. An analytical model permits a simple qualitative understanding of the effects of the plasma-induced defects, the factors that affect the QWI process, and the general correlations of the inductively coupled plasma exposure effect on a QW's bandgap shift.

This paper is organized as follows. The experiments of Ar plasma exposure both with and without inductively coupled plasma application on InGaAs–InGaAsP QW structures is introduced in Section II. The theoretical basis for the plasma-induced defects and the semi-empirical model used in calculating the interdiffusion coefficient of the mobile point defects to promote intermixing are described in Section III. The results obtained from both the experiments and the model are then presented and discussed in Section IV. The plasma-induced defect model is then curve-fitted with the experiment data. Section V summarizes the main conclusions of this paper.

II. Experiments

The lattice-matched InGaAs–InGaAsP QW samples used in the present investigation were grown by metal–organic vapor phase epitaxy on (100) oriented n^+-type S-doped InP substrate with an etch-pit density below 1000 cm^{-2} [13]. Instead of a single QW structure, the present structure consists of five periods of 5.5-nm $In_{0.53}Ga_{0.47}As$ QWs with 12-nm InGaAsP barriers. The active region is sandwiched by a step-graded index waveguide core consisting of InGaAsP confining layers. The thickness of these confining layers is 50 and 80 nm, respectively. The structure was completed by an upper cladding InP layer of 1.37 μm with Zn doping of $7.3 \cdot 10^{17}$ cm^{-3}. The contact layer consists of 50-nm InGaAsP (Zn-doped of $2 \cdot 10^{18}$ cm^{-3}) and 100-nm InGaAs (Zn-doped of $1.8 \cdot 10^{19}$ cm^{-3}).

The plasma source generator ICP 180 used in the experiments was a Plasmalab System 100, which was built by Oxford Instruments. The system uses inductive coil to generate high-density "remote" plasma with no direct contact between the plasma and the substrate. The 13.56-MHz radio frequency (RF) and ICP power supply can provide the independent control on ion bombardment energy and ion current density with the operating powers up to 500 and 3000 W, respectively. The chamber base pressure is maintained at $5 \cdot 10^{-5}$ torr. The ICP chamber is equipped by a water circulator to maintain the table temperature at 60 °C. The thermocouple, which is attached on the ICP chamber's wall, shows an increase up to 3 °C during the intial plasma strike and reaches steady state temperature in less than 10 s. The ICP system is equipped with the He-back side cooled electrode with a quartz as a wafer susceptor. The QW samples were placed at the silicon substrate to provide a fairly large (168 W/mK) heat conduction. The ICP parameter settings for the experiments were optimized using Taguchi's method [14], i.e., 100-sccm Ar flow rate, 80-mtorr chamber pressure, and 480-W RF power.

After Ar plasma exposure, the samples were annealed at 600 °C for 4 min in a rapid thermal processor (RTP) in a nitrogen atmosphere, which is sufficient for a complete propagation of the created near-surface mobile defects through the active QW region. Two fresh pieces of GaAs proximity caps were used to provide an arsenic over-pressure environment during the annealing process and further to prevent the sample surface from arsenic outdiffusion. Photoluminescence (PL) measurements were then performed to assess the degree of bandgap shift. The PL measurements were carried out using an Nd:YAG laser (1.064 μm) for excitation, a monochromator, and a TE-cooled InGaAs photodetector associated with an SR-830 lock-in amplifier. The as-grown sample, which refers to the QW sample with neither exposure or annealing process, showed a PL peak at 1.51 ± 0.02 μm at room temperature (RT) and 1.43 ± 0.02 μm at 77 K. A control sample, which was annealed to determine the thermal shift without exposure to plasma, had bandgap blue-shift of 6.5 nm as compared to the as-grown sample.

III. Theoretical Model

The majority of the impinging ions of Ar plasma is stopped within the first few atomic monolayers of material and may cause cause lattice disruption [15] and damage up to a depth of a few tens of nanometers [16]. A number of experiments have confirmed that defects generated from low-energy ion (with hundreds of electronvolts of ion impact energy) processes can penetrate more than 100 nm into the substrate [16], [17]. The very short duration of plasma exposure (less than 10 min) is sufficient to raise the formation probability of surface defects and thus cause surface damage to a semiconductor substrate even with very small ion bombardment energy from 10 to 100 eV [18]. Instead of the radiation-enhanced motion defects [18], the channeling mechanism at this small ion bombardment energy has been identified as the primary mechanism causing defects deep within the plasma-exposed crystalline material, with diffusion possibly modifying the final defect distribution [20]. Both the electrical and optical measurement techniques have been used to study the plasma-induced defects after exposure, including a damage detection technique using a QW as a probe [21]. This technique is based on the understanding that the luminescence from the as-grown sample is dominated by the radiative recombination, whereas the plasma-induced defects in the QW active region will contribute to the rise of nonradiative recombination. Therefore, a decrease in PL intensity will be observed from the plasma-exposed region. From the reported results, the plasma-induced defects on the near surface of samples can be summarized as follows.

1) The magnitude of the created defects increases with the plasma exposure time but the damage depth remains constant [21], [22].
2) The magnitude of created defects is expected to saturate after a long exposure time to the plasma [23].

3) The magnitude of the created defects is higher in the low etch-rate process than that in the higher etch-rate process [21], [24].
4) The magnitude of the created defects is higher in the high-density plasma rather than in the low-density plasma [11], [20].

The near-surface defects created during plasma exposure propagate into the QW region during the annealing step. The arrival of defects in the QW region enhancing the interdiffusion of the group III and group V species promotes the intermixing, widens the bandgap, and results in the blue-shift of PL emission. In the unexposed samples, the annealing step contributes a small bandgap shift, which could be attributed to the presence of the grown-in defects on the QW interfaces during growth. Our semi-empirical interdiffusion model is based on the plasma-induced defects model that the amount of point defects that can induce the QWI process are limited and saturate exponentially with the plasma exposure time. We assume that the point defects density created during the plasma exposure is uniform in the vicinity of the QWs upon annealing. This approximation is made based on the fact that the QW width layers are very thin, i.e., 5.5 nm, as compared to the distance of the QW region from the sample surface. It is known that interdiffusion of the defects in the plasma process is strongly affected by temperature. For the analysis performed in our model, we take into account the total amount of defects generated on the sample surface, thus the defect distribution due to temperature variation during plasma exposure will not affect our model.

The extent of the intermixing degree in the QW region can be characterized using the interdiffusion coefficient of certain atomic species D_{QW} as a function of the total number of near surface point defects [26] as follows:

$$D_{\mathrm{QW}} = \sigma \lambda_D^2 \Gamma_D = (\sigma_0 + \sigma_E)\, \lambda_D^2 \Gamma_D \tag{1}$$

where σ_0 is the equilibrium number concentrations of mobile point defects, σ_E is the excess number concentrations of mobile point defects created by the high-density plasma application, Γ_D is the hopping frequency of the point defect, and λ_D is the mean free path of the point defect. Since the point defect creation is a random interaction with atomic lattice, the probability of defect creation is proportional to the number of possible defects that can be created. Assuming that the lattice can only accommodate a certain maximum number concentrations of defects (σ_{sat}) [27], the rate of point defect creation due to high-density plasma enhancement can then be expressed as

$$\frac{d\sigma_D}{dt} = k(\sigma_{\mathrm{sat}} - \sigma_E) \tag{2}$$

where t is the plasma exposure time and k is the point defect creation constant, which indicate the rate of defects creation per unit exposure time. This parameter k depends on the plasma radiation intensity. Solving this differential equation from (2) gives

$$\sigma_E = \sigma_{\mathrm{sat}} \left(1 - e^{-kt}\right). \tag{3}$$

This relationship intuitively shows that the rate of number concentrations of defects decreases as the exposure time increases. Most of the defects will be created in the early stage of exposure. As the defects start to build up, there will be fewer defects created subsequently. This agrees with the experimental observation that the degree of intermixing is not as dependent on plasma exposure time after a long exposure in the plasma-enhanced QWI process. The saturated amount of mobile point defects depends on the nature of the plasma, including the RF-induced dc bias condition, such that the value will be different with the change of inductively coupled plasma power.

Considering the above points, (1) can be expressed as

$$D_{\mathrm{QW}} = \sigma_0 \lambda_D^2 \Gamma_D + \sigma_{\mathrm{sat}} \lambda_D^2 \Gamma_D (1 - e^{-kt}) = D_0 + D_E (1 - e^{-kt}) \tag{4}$$

where D_0 is the interdiffusion coefficient in thermal equilibrium and D_E is the interdiffusion coefficient enhanced by the excess mobile point defects due to plasma exposure. Both parameters are associated with the QW material, annealing condition, and plasma properties. D_{QW} is also temperature-dependent and can be approximated using the Arrhenius equation.

The value of the interdiffusion coefficients and their related parameters can be deduced from the PL measurement results after solving the interdiffused QW bound states calculation. The subband states in the QW are calculated separately for electron (E) and heavy hole (HH)/ light hole (LH) by solving the Ben Daniel Duke's equation from the one-dimensional (1-D) Schrödinger-like equation [28] with a z-position-dependent effective mass on the interdiffused composition profile.

The problem is formulated by modeling the interdiffusion process in the QW layer. Assuming Fick's law and concentration-independent interdiffusion coefficient (D_{QW}), the concentration profile of groups III and V in the $\mathrm{In_xGa_{1-x}As_yP_{1-y}}$ QWs can be derived in term of superposition of error functions [29]. The band edge interdiffusion profile including the graded-index layer is modeled based on the assumption of interdiffusion that obeys the linear Fick's law. L_d is the interdiffusion length given by $L_d = \sqrt{D_{\mathrm{QW}} t_a}$, where t_a is the interdiffusion time normally associated with annealing time. The extent of the interdiffusion in the QW can be characterized by two parameters: interdiffusion length of group III elements, L_{dIII} and interdiffusion length of group V elements L_{dV}. In our calculation, the interdiffused QWs are characterized using an identical interdiffusion length of group III and group V atoms [30]. This implies that the interdiffusion rates of anions and cations are considered to be identical during intermixing process ($L_{\mathrm{dIII}} = L_{\mathrm{dV}}$). This assumption of lattice-matched conservation is supported with the experimental finding concerning the intermixing effect of InGaAs–InP QWs using Raman spectroscopy [31], secondary ion mass spectroscopy [32], and high-resolution X-ray diffraction measurement [33]. The atomic compositional profiles, x and y, are no longer independent but related as $x = 1 - 4.07y$. It gives a lattice-matching condition with the InP substrate within $|\Delta a/a| < 0.032\%$ [34], where a is the lattice constant. Transforming the differential equation into an eigen-value matrix, called the finite difference eigen value (FDEV) method [35], is used to solve the Ben-Daniel Duke's equation. In this way, the QW interband transition energies can be calculated. The ground state transitional energy (E1-HH1) that corresponds to the peak excitonic wavelength were fitted to the measured PL peak en-

ergies of intermixed samples by adjusting the value of L_d, thus L_d and D_{QW} can be determined.

IV. Results and Discussion

In order to study the effect of inductively coupled Ar plasma exposure, a set of QW samples from the same wafer was exposed under Ar plasma in an ICP chamber with a pure RF power of 480 W. The ICP power was turned off during plasma exposure. The corresponding RF-induced dc bias was -840 V. Under this condition (ICP power $= 0$ W), the ionic species in the plasma sheath region is accelerated at normal incidence by electric field and is expected to strongly induce highly energetic ion bombardment damage. The plasma exposure to the QW samples under this condition leads to intermixing due to the ion bombardment-induced damage. The PL spectrum at 77 K as a function of exposure time is plotted in Fig. 1, including the control sample for comparison.

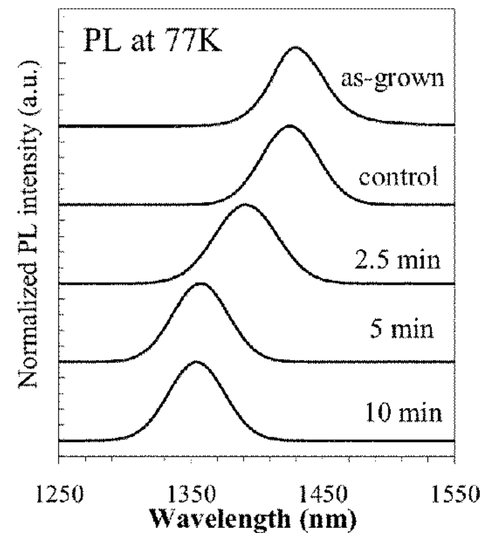

Fig. 1. Plot of normalized PL spectra at 77 K for different Ar exposure times under pure RF power (without inductively coupled Ar plasma application). The samples were exposed under pure RF power and subsequently annealed at 600 °C for 4 min.

The annealing was done below the critical annealing temperature from the thermal stability test (600 °C for 4 min), beyond which the as-grown sample will experience appreciable bandgap shift. The control sample underwent a 6.5-nm bandgap shift as compared to the as-grown sample, which is mainly attributed to thermal shift after annealing. It can be observed from the curve that the bandgap of the samples subject to longer exposure time have been shifted to higher energy after annealing. The sample after 10 min of exposure showed the most blue-shifted PL spectra with a peak of 1354 nm. The bandgap shift from PL spectra saturates after 10 min of exposure at about 84 nm. This can be understood that most of the defects will be created in the early stage of Ar exposure and, as the defects start to build up, fewer defects will subsequently be created. The bandgap shift achieved using pure RF power in this experiment is comparable to similar Ar plasma QWI using a conventional parallel-plate RIE machine with similar RF power in the InGaAs–InGaAsP QW structures [36]. For the control and intermixed samples, only minimal linewidth broadening was observed as the exposure time and intermixing process increases. Thus, no significant degradation of optical properties has occurred in the QW samples.

In this session, we investigate the effects of QWI using the presence of inductively coupled Ar plasma by applying ICP power. A Taguchi's method requires high RF power together with low ICP power for a high bandgap shift with small linewidth broadening [12]. A comparative study was made to identify the intermixing effect by using the inductively coupled plasma with the increase of ICP power from 0 to 500 W and keeping constant RF power at 480 W. Fig. 2 shows the optimum PL shift at RT and corresponding self RF-induced dc bias of the ICP machine versus ICP power. The application of ICP power reduces RF-induced dc bias but promotes a higher bandgap shift. The RF-induced dc bias reduction leads to less ion bombardment-induced damage with the increase in ion current density. This result implies that the presence of higher plasma density from inductively coupled Ar plasma plays an important role in enhancing QWI process [15]. Our results are supported by the earlier experimental studies using reactive ion beam etching [37], [38], which showed that the high plasma ion density and the high intensity of plasma radiation together with ion bombardment could enhance the defect diffusion and may cause the deeper penetration in the semiconductors. Upon annealing, the enhanced mobile point defects will propagate into the QW region to promote intermixing between barriers and QWs. Optimum bandgap shift using ICP power with minimum linewidth broadening was obtained at an ICP power of 500 W and an RF-induced dc bias of -730 V. The bandgap of the QW has been blue-shifted by as large as 112 nm after plasma exposure for 5 min using 500 W of ICP power.

Earlier work reported that the defect enhancement takes place due to a radiation-enhanced diffusion process [39] and the high-density of atomic ions in the discharge during exposure [18]. Chen *et al.* recently found that the damage depth seemed to increase with the illumination intensity and attributed this to enhancing the defect diffusion on top of any channeling effect [37]. It was determined that the generation of high-energy photons in the vacuum ultraviolet (VUV) range (4–30 eV) as high as 1 $\mathrm{mW/cm^2}$ is possible to introduce radiation damage on semiconductor devices in the plasma chamber [40]. This radiation-enhanced damage can be attributed due to the net effect of both electron–hole recombination via electron phonon coupling and an excess flux of phonons or due to the net effect of the plasma radiation and ion bombardment. The radiation damage in the VUV range to affect the intermixing were studied by irradiating the QW samples using the UV light source of a peak wavelength of 365 nm from a Q2001CT UV-mask contact aligner (Quintel Corporation) at a power intensity irradiance of 1.5 $\mathrm{mW/cm^2}$ [41]. There was no bandgap shift from the PL measurements due to the UV source irradiance, after exposure up to 15 min and subsequent annealing. The exposure using ICP power of 500 W without the application of RF-induced dc bias on the QW sample enables the VUV radiation damage effect created on the QW sample. The samples exposed

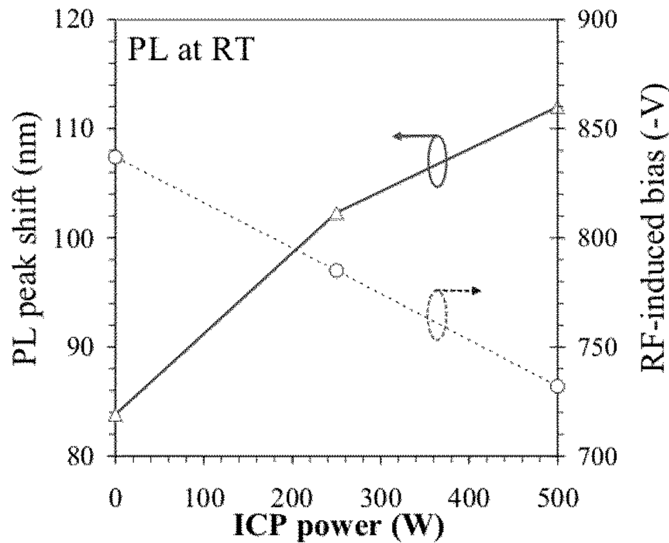

Fig. 2. Optimum PL blue-shift (open triangles) and RF-induced dc bias (open circles) as a function of ICP power. The condition was taken at a constant RF power of 480 W for up to 15 min of exposure time.

up to 15 min and subsequent annealing resulted in no observable PL peak shift.

To further investigate the effect of inductively coupled plasma, a collisonal sheath global discharge cylindrical model [42] is adopted to calculate the Ar plasma properties in ICP discharge. We calculate the steady-state ion current density (J_i) and the sheath voltage (V_s) at a constant RIE power of 480 W. It should, however, be pointed out the plasma density is slightly overestimated in our calculation as we have assumed that all the RF power is fully absorbed by the plasma. The ion bombardment voltage is roughly equal to V_s, and RF-induced dc bias decreases with the increase in ICP power from 0 to 500 W as a result, ranging from V_s =840 to 620 V. The J_i increases linearly from about 0.36 to 1.2 mA/cm^2. This corresponds to a dose rate of $6.7 \cdot 10^{17}$ to $2.2 \cdot 10^{18}$ $ions/cm^2$ for a 5-min plasma exposure, which is several orders larger than the traditional ion-implantation method [3]. The impact intensity by a high ion dose at an ICP power of 500 W is about 550 mW/cm^2 for 5-min plasma exposure, which is three orders of magnitude higher than the typical VUV Ar irradiance level of 0.96 mW/cm^2 with the integrated photon flux of $3.64 \cdot 10^{13}$ $cm^{-2} \cdot s^{-1}$ in the ECR chamber [40]. Thus, we believe that the high-dose ion exposure due to the inductively coupled plasma application has a more significant effect on enhancing the degree of intermixing in the ICP chamber as compared to the presence of plasma radiation in the discharge. This is similar to a relevant report for damage enhancement in the ECR machine at a higher ion dose as compared to the RIE machine [18], [38].

The five-period lattice-matched InGaAs–InGaAsP QW laser structure will be considered for theoretical analysis in various stages of the Ar exposure process. The calculated constituent atom compositional profiles of In, Ga, As, and P across the QW region after intermixing are shown in Fig. 3. It can be seen that the compositional profiles change from the abrupt one to the

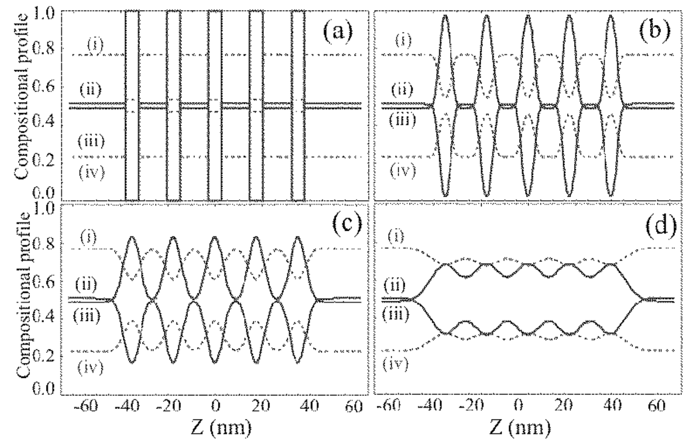

Fig. 3. Composition profiles of identical interdiffusion InGaAs–InGaAsP QW structures of each constituent atom compositional profiles. (i) In. (ii) P. (iii) As. (iv) Ga as the interdiffusion lengths vary at (a) $L_d = 0$ Å, (b) $L_d = 10$ Å, (c) $L_d = 20$ Å, (d) $L_d = 40$ Å. The dotted lines represent the group III atoms and the solid lines represent the group V atoms.

error function profiles for all the quaternary atoms as the interdiffusion length increases. The Ga and As atoms in the wells diffuse into the $In_{0.77}Ga_{0.23}As_{0.49}P_{0.51}$ barriers while the In atoms and the P atoms in the barrier move into the $In_{0.53}Ga_{0.47}As$, resulting in the final InGaAsP–InGaAsP interface after intermixing. For longer interdiffusion length ($L_d > 40$ Å), the compositional profiles tend to be uniform across the structures, resembling the bulk-like profiles.

The strain profiles were calculated to validate the assumption of the lattice-matching condition after intermixing due to the change of atom distribution across the QW. As shown in Fig. 4, the very small tensile strain ($< 0.0018\%$) is present in the barrier near the interface since the unintermixed $In_{0.77}Ga_{0.23}As_{0.49}P_{0.51}$ barrier lattice constant has a larger value than the intermixed InGaAsP lattice constant in the barrier after intermixing. No strain is observed in the barrier center during early levels of intermixing ($L_d < 10$ Å). The compressive strain appears in the well center, since the unintermixed $In_{0.53}Ga_{0.47}As$ lattice constant and the intermixed InGaAsP lattice constant in the wells is always larger than the $In_{0.77}Ga_{0.23}As_{0.49}P_{0.51}$ lattice constant in the barrier. The increase of lattice constant is attributed by the compositional change in the wells, which corresponds to the increase of the In and P contents and the decrease of the Ga and As contents coherently. The largest compressive strain is present in the unintermixed $In_{0.53}Ga_{0.47}As$ wells, and the strain becomes smaller as the interdiffusion length increases. The compressive strain for the same interdiffusion length exhibits the largest value in the well centers for the intermixed QWs and has the minimum value in the wells near the interface since the well centers have fewer In and P atoms (also more Ga and As atoms) than those in the wells near the interface. However, both the tensile strain in the barrier near the interface and the wells show that the lattice-matching condition of the QWs is maintained for an intermixed structure (in-plane strain for all points is still less than that for the lattice-matched condition, 0.032%). For longer interdiffusion lengths, the strain will be smaller across the wells and barriers since the compositional profile tends to

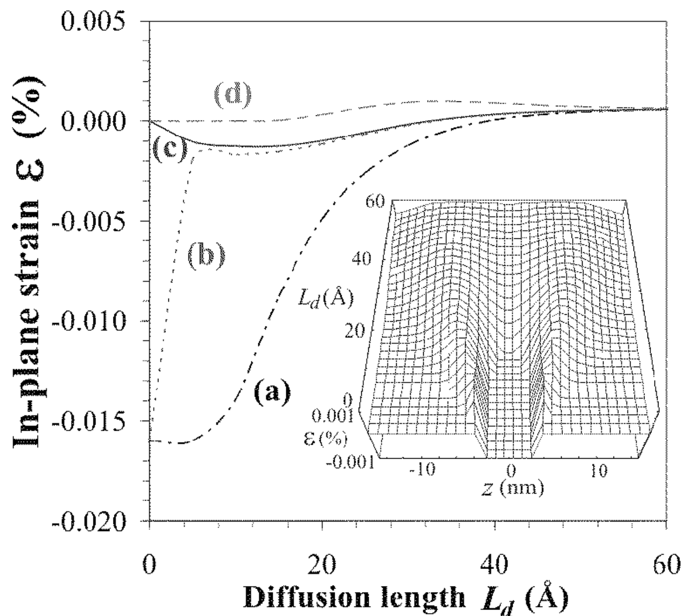

Fig. 4. In-plane strain variation of identical interdiffusion versus interdiffusion length across a QW structure on the different positions: (a) well center, (b) the well close to the interface, (c) the barrier close to interface, and (d) the barrier center. The inset shows the strain distribution across a QW and quantum barrier as a function of growth direction (z). $z = 0$ denotes the center of the QW.

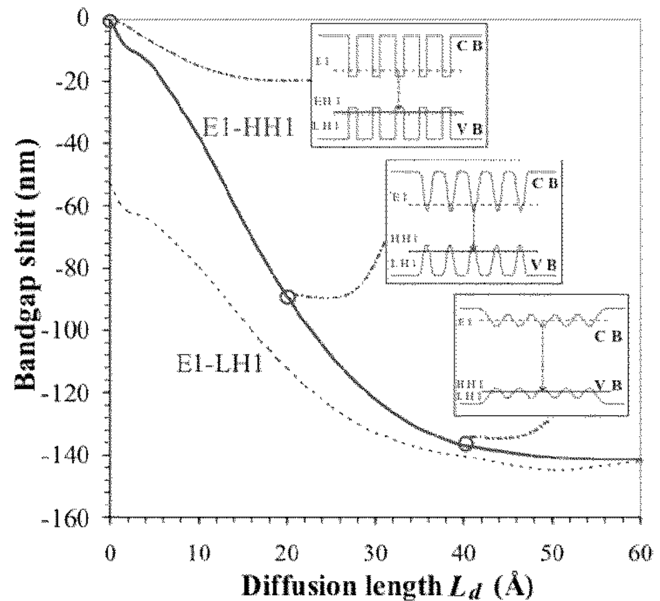

Fig. 5. Calculated RT ground state exciton transition energy (E1-HH1 and E1-LH1) with respect to PL peak of an as-grown sample as a function of single interdiffusion length L_d. The inset shows the corresponding confinement profile for both the conduction and valence bands.

be uniform, which is like the so-called bulk-like profiles, as mentioned earlier.

The ground state E1-HH1 and E1-LH1 transition energies as a function of the single interdiffusion length are shown in Fig. 5. The E1-HH1 calculation of the bound states' transition energy is related to the PL emission of the QW samples, and this is a result of compositional profile change. Due to the effect of small in-plane strain, the changes of bulk bandgap energy causes the shift in transition energies rather than the change of the hydrostatic and shear deformation potential energies. The plot gives very important information regarding the maximum possible bandgap or wavelength shift that can be obtained from this QW structure by the intermixing process. As the interdiffusion length increases, the E1-HH1 transition energy also increases, which is known as the blue-shift phenomenon, reported recently for the same material of interdiffused InGaAs–InGaAsP QW using IID [2], [3], [8], FIB [4], IFVD [5], sputter silica [6], and LID [7]. It can be noted that significant intermixing occurs up to an interdiffusion length of 50 Å. Beyond this, the intermixing effect is less pronounced. This effect can be observed in the experiment as the "saturation phenomena," i.e., there are fewer shifts in the exciton peak at a high degree of intermixing. This result agrees with the previous experimental observations that samples exposed to Ar plasma for longer exposure time tend to saturate at a certain maximum shift in wavelength. It can be observed that both E1-HH1 and E1-LH1 excitons are shifted to the shorter wavelength; this shift is much larger for E1-HH1 than for E1-LH1. A change in interdiffusion length from 0 to 50 Å corresponds to a change in the E1-HH1 transition energy of about 85.5 meV, which represents a shift to a shorter wavelength of about 140 nm with respect to the E1-HH1 transition energy of the as-grown sample, whereas the corresponding light hole transition energy changes by about 58 meV, representing a shift to shorter wavelengths of about 92 nm with respect to the E1-LH1 transition energy of as-grown samples. The inset shows the corresponding confinement profiles of electrons and holes in the QW region. The change from the abrupt profile to the graded profile indicates that there is a small amount of confinement loss.

From the E1-HH1 ground-state transition energy curve in Fig. 5, the correspondence interdiffusion length and the interdiffusion coefficient can be deduced from the experimental data of the intermixed samples without inductively coupled plasma energy (low-density plasma) and with inductively coupled plasma energy (high-density plasma). The deduced interdiffusion coefficient was fitted to the semi-empirical model of the interdiffusion coefficient in (4) upon annealing to promote the intermixing. From (4), the interdiffusion coefficients of point defect propagation increase with the Ar exposure time qualitatively. Fig. 6 shows the comparison of interdiffusion coefficients between the experimental data and the curve-fitted results using our semi-empirical model. The interdiffusion coefficients from experimental data can be fitted well with our model with the parameters as shown in the inset. The small increase of k with respect to the ICP application is as expected, which is attributed to the increase in the radiation intensity from the high plasma density. At a short exposure time, the diffusivity increases rapidly, corresponding to the most defects created in the early stage of Ar exposure. The interdiffusion coefficient saturates after long exposure times at the interdiffusion value at $D_{\rm QW} \sim 1.5 \cdot 10^{-16}$ cm^2/s and $D_{\rm QW} \sim 3.0 \cdot 10^{-16}$ cm^2/s for ICP power at 0 and 500 W, respectively. The application of 500-W inductively coupled plasma enhances the defect interdiffusion coefficient twice as much as the application with no ICP power. This diffusivity saturation implied that the amount of bandgap shift saturates for a very long exposure time. The inductively coupled

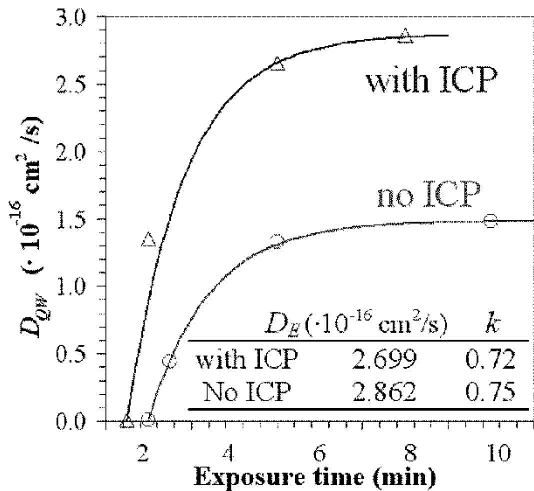

Fig. 6. Interdiffusion coefficients between QWs and barriers, deduced from the experimental bandgap shift, versus exposure times for plasma exposure without inductively coupled plasma (open circle) and with inductively coupled plasma of 500-W ICP power (open triangle). The solid line represents the best fit from the theoretical model. The RF power was set at 480 W for these plasma conditions.

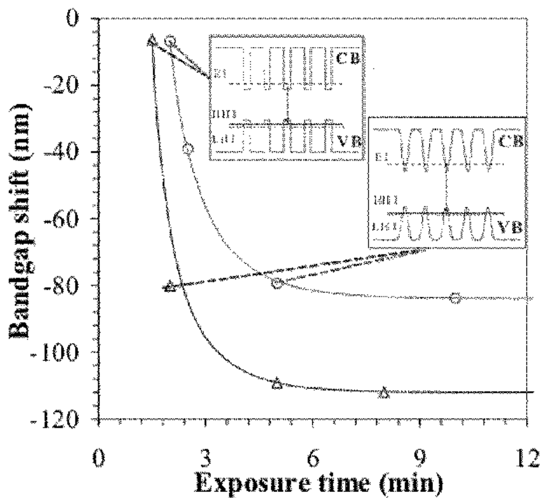

Fig. 7. Bandgap shifts are plotted as a function of plasma exposure time. The experimental bandgap shift obtained in this work without inductively coupled plasma (open circles) and with inductively coupled plasma of 500-W ICP power (open triangles). The solid line represents the best fit from the theoretical model. The RF power was set at 480 W for these plasma conditions. The inset shows the deduced confinement profile of both conduction band and valence band.

plasma application, which results in the high ion density and the high intensity of plasma radiation, may cause the enhancement in diffusivity.

The experimental data of intermixed samples are then interpreted using the model in order to identify the enhanced QWI process with the application of inductively coupled Ar plasma. Fig. 7 shows a comparison between the best-fit theoretical model and the experimental results of blue-shift in wavelength as a function of Ar plasma exposure time. The interdiffusion model is curve fitted to the existing data, implying that the intermixing processes obey the behavior that the model assumes. For an exposure time of 5 min or below, the relationship between the bandgap energy shift and time is linear. However, for longer exposure time, this relationship becomes nonlinear. Preliminary interdiffusivity calculations have ruled out the possibility of this saturation effect being due to the complete intermixing induced by the propagation of mobile point defects and thus imply that the interdiffusion mechanisms take on a different behavior in this regime. The inclusion of enhanced defects interdiffusion due to inductively coupled plasma according to the semi-empirical model, even at a very simple level, seems to provide good agreement with the experimental results.

V. Conclusion

QWI has been demonstrated using Ar plasma exposure in an ICP system. The degree of intermixing increases with exposure time and with application of inductively coupled Ar plasma. The plasma-induced defect model predicts that the magnitude of plasma-induced defects is higher for the high-density plasma exposure with the application of the inductively coupled plasma. Using the semi-empirical model, a substantial progress has been made in understanding the mechanism of the increase in the material bandgap energy using ICP exposure. The experimental data were well supported and explained by our theoretical model. According to our model, the degree of intermixing increases and saturates as the exposure time increases, which is in good agreement with the observation from experiments. The achievement of higher intermixing degree by the application of inductively coupled Ar plasma has been primarily due to the inductively coupled plasma-enhanced interdiffusion of mobile point defects. The model serves as a good simulation program to study the intermixing mechanism and further to optimize the plasma-enhanced QWI process for the fabrication of PICs.

References

[1] J. H. Marsh, "Quantum well intermixing," *Semicond. Sci. Technol.*, vol. 8, pp. 1136–1155, 1993.

[2] V. Aimez, J. Beauvais, J. Beerens, D. Morris, H. S. Lim, and B. S. Ooi, "Low-energy ion-implantation-induced quantum-well intermixing," *IEEE J. Select. Topics Quantum Electron.*, vol. 8, pp. 870–879, 2002.

[3] S. Charbonneau, E. S. Koteles, P. J. Poole, J. J. He, G. C. Aers, H. Haysom, M. Buchanan, Y. Feng, A. Delage, F. Yang, M. Davies, R. D. Goldberg, P. G. Piva, and I. V. Mitchell, "Photonic integrated circuits fabricated using ion implantation," *IEEE J. Select. Topics Quantum Electron.*, vol. 4, pp. 772–793, 1998.

[4] J. P. Reithmaier and A. Forchel, "Focused ion-beam implantation induced thermal quantum well intermixing for monolithic optoelectronic device integration," *IEEE J. Select. Topics Quantum Electron.*, vol. 4, pp. 595–605, 1998.

[5] S. K. Si, D. H. Yeo, K. H. Yoon, and S. J. Kim, "Area selectivity of InGaAsP-InP multiquantum-well intermixing by impurity-free vacancy diffusion," *IEEE J. Select. Topics Quantum Electron.*, vol. 4, pp. 619–623, 1998.

[6] S. P. McDougall, O. P. Kowalski, C. J. Hamilton, F. Camacho, B. Qiu, M. Kee, R. M. De La Rue, A. C. Bryce, and J. H. Marsh, "Monolithic integration via a universal damage enhanced quantum well intermixing technique," *IEEE J. Select. Topics Quantum Electron.*, vol. 4, pp. 636–646, 1998.

[7] B. C. Qui, A. C. Bryce, R. M. D. L. Rue, and J. H. Marsh, "Monolithic integration in InGaAs-InGaAsP multiquantum-well structure using laser processing," *IEEE Photon. Technol. Lett.*, vol. 10, pp. 769–771, 1998.

[8] E. J. Skogen, J. S. Barton, S. P. Denbaars, and L. A. Coldren, "A quantum-well-intermixing process for wavelength-agile photonic integrated circuits," *IEEE J. Select. Topics Quantum Electron.*, vol. 8, pp. 863–869, 2002.

[9] B. S. Ooi, A. C. Bryce, and J. H. Marsh, "Integration process for photonic integrated circuits using plasma damage induced layer intermixing," *Electron. Lett.*, vol. 31, pp. 449–451, 1995.

[10] T. C. L. Wee, B. S. Ooi, T. K. Ong, Y. L. Lam, Y. C. Chan, and G. I. Ng, "Novel quantum well intermixing in InGaAs-InGaAsP laser structure using argon plasma exposure," in *Conf. Dig. IEEE Lasers and Electro-Optics Europe*, 2000, pp. 234–234.

[11] H. S. Djie, T. Mei, J. Arokiaraj, and P. Thilakan, "High-density plasma enhanced quantum well intermixing in InGaAs/InGaAsP structure using argon plasma," *Jpn. J. Appl. Phys.*, vol. 41, pp. L867–L868, 2002.

[12] H. S. Djie, C. Sookdhis, T. Mei, and J. Arokiaraj, "Photonic integration using inductively coupled argon plasma enhanced quantum well intermixing," *Electron. Lett.*, vol. 38, pp. 1672–1673, 2002.

[13] H. S. Lim, V. Aimez, B. S. Ooi, J. Beauvais, and J. Beerens, "A novel fabrication technique for multiple-wavelength photonic-integrated devices in InGaAs-InGaAsP laser heterostructures," *IEEE Photon. Technol. Lett.*, vol. 14, pp. 594–596, 2002.

[14] D. Leong, H. S. Djie, and P. Dowd, "A new quantum well intermixing technique using inductively-coupled argon plasma on InGaAs/InGaAsP laser structures," in *Proc. Int. Conf. IEEE 14th Indium Phospide and Related Materials (IPRM)*, 2002, pp. 319–3122.

[15] H. S. Djie, J. Arokiaraj, and T. Mei, "Inductively coupled argon plasma enhanced quantum well intermixing in InGaAs/InGaAsP laser structure," in *Proc. IEEE 29th Int. Symp. Compound Semiconductors (ISCS)*, Lausanne, Switzerland, Oct 7–10, 2002, Tu-P-35.

[16] D. L. Green, E. L. Hu, and N. G. Stoffel, "Effect of superlattices on the low-energy ion-induced damage in GaAs/Al(Ga)As structures: Channeling or diffusion?," *J. Vac. Sci. Technol. B*, vol. 12, pp. 3311–3316, 1994.

[17] C. H. Chen, D. G. Yu, E. L. Hu, and P. M. Petroff, "Photoluminescence studies on radiation enhanced diffusion of dry-etch damage in GaAs and InP materials," *J. Vac. Sci. Technol. B*, vol. 14, pp. 3684–3687, 1996.

[18] Z. W. Deng, R. W. M. Kwok, W. M. Lau, and L. L. Chao, "Bandgap state formation in InP (110) induced by 10 and 100 eV argon ion bombardment," *J. Appl. Phys.*, vol. 86, pp. 3676–3681, 1999.

[19] M. Rahman, "Channeling and diffusion in dry-etch damage," *J. Appl. Phys.*, vol. 82, pp. 2215–2224, 1997.

[20] M. Rahman, L. G. Deng, J. Van Den Berg, and C. D. W. Wilkinson, "Minimization of dry etch damage in III–V semiconductors," *J. Phys. D: Appl. Phys.*, vol. 34, pp. 2792–2797, 2001.

[21] B. S. Ooi, A. C. Bryce, C. D. W. Wilkinson, and J. H. Marsh, "Study of reactive ion etching-induced damage in GaAs/AlGaAs structures using a quantum well intermixing probe," *Appl. Phys. Lett.*, vol. 64, pp. 598–600, 1994.

[22] H. F. Wong, D. L. Green, T. Y. Liu, D. G. Lishan, M. Bellis, E. L. Hu, P. M. Petroff, P. O. Holtz, and J. L. Merz, "Investigation of reactive ion etching induced damage in GaAs-AlGaAs quantum well structures," *J. Vac. Sci. Technol. B*, vol. 6, pp. 1906–1910, 1988.

[23] D. Lootens, P. Van Daele, P. Demeester, and P. Clauws, "Study of electrical damage in GaAs induced by $SiCl_4$ reactive ion etching," *J. Appl. Phys.*, vol. 70, pp. 221–224, 1991.

[24] B. S. Ooi, S. E. Hicks, A. C. Bryce, C. D. W. Wilkinson, and J. H. Marsh, "Study of C_2F_6 overetch induced damage and the effects of overetch on subsequent $SiCl_4$ etch of GaAs/AlGaAs," *J. Appl. Phys.*, vol. 77, pp. 4961–4966, 1995.

[25] R. J. J. Visser, "Determination of the power and current densities in argon and oxygen plasmas by in situ temperature measurements," *J. Vac. Sci. Technol. A*, vol. 7, pp. 189–194, 1989.

[26] R. J. Borg and G. J. Dienes, *Solid State Diffusion*. Boston, MA: Academic, 1988.

[27] O. Gunawan, T. K. Ong, Y. W. Chen, B. S. Ooi, Y. L. Lam, Y. Zhou, and Y. C. Chan, "A theoretical analysis of quantum well intermixing using the pulsed laser irradiation technique in InGaAsrInGaAsP laser structure," *J. Surface Coatings Technol.*, vol. 130, pp. 116–121, 2000.

[28] D. J. Ben-Daniel and C. B. Duke, "Space-charge effects on electron tunneling," *Phys. Rev.*, vol. 152, pp. 683–692, 1966.

[29] T. E. Schlesinger and T. Kuech, "Determination of the interdiffusion of Al and Ga in undoped (Al,Ga)As/GaAs quantum wells," *Appl. Phys. Lett.*, vol. 49, pp. 519–521, 1986.

[30] H. Peyre, F. Alsina, J. Camassel, J. Pascual, and R. W. Glew, "Thermal stability of InGaAs/InGaAsP quantum wells," *J. Appl. Phys.*, vol. 73, pp. 3760–3768, 1993.

[31] S. J. Yu, H. Asahi, S. Emura, and S. I. Gonda, "Raman scattering study of thermal interdiffusion in InGaAs/InP superlattice structures," *J. Appl. Phys.*, vol. 70, pp. 204–208, 1991.

[32] D. H. Yeo, K. H. Yoon, and S. J. Kim, "Characteristics of intermixed InGaAs/InGaAsP multi-quantum-well structure," *Jpn. J. Appl. Phys.*, vol. 39, pp. 1032–1034, 2000.

[33] F. Bollet, W. P. Gillin, M. Hopkinson, and R. Gwiliam, "On the diffusion of the lattice matched InGaAs/InP microstructures," *J. Appl. Phys.*, vol. 93, pp. 3881–3885, 2003.

[34] S. Adachi, "Material parameters of $In_{1-x}Ga_xAs_yP_{1-y}$ and related binaries," *J. Appl. Phys.*, vol. 53, pp. 8775–8792, 1982.

[35] H. S. Djie, S. L. Ng, O. Gunawan, P. Dowd, V. Aimez, J. Beauvais, and J. Beerens, "Analysis of strain-induced polarization insensitive integrated-waveguides fabricated using ion implantation-induced intermixing," *Proc. Inst. Elect. Eng.*, pt. J, vol. 149, pp. 138–144, 2002.

[36] D. Leong, H. S. Djie, and L. K. Ang, "Quantum well intermixing using argon plasma generated in a reactive-ion etching system on InGaAs/InGaAsP laser structures," in *Proc. Int. Conf. IEEE/LEOS Workshop Fiber and Optical Passive Components*, 2002, pp. 148–152.

[37] C. H. Chen, D. L. Green, E. L. Hu, J. P. Ibbetson, and P. M. Petroff, "Radiation enhanced diffusion of low energy ion-induced damage," *Appl. Phys. Lett.*, vol. 69, pp. 58–60, 1996.

[38] S. Murad, M. Rahman, N. Johnson, S. Thoms, S. P. Beaumont, and C. D. W. Wilkinson, "Dry etching damage in III–V semiconductors," *J. Vac. Sci. Technol. B*, vol. 14, pp. 3658–3316, 1996.

[39] L. G. Deng, M. Rahman, and C. D. W. Wilkinson, "Enhanced damage due to light in low-damage reactive ion etching processes," *Appl. Phys. Lett.*, vol. 76, pp. 2871–2873, 2001.

[40] C. Cisamaru and J. L. Shohet, "Plasma vacuum ultraviolet emission in an electron cyclotron resonance etcher," *Appl. Phys. Lett.*, vol. 74, pp. 2599–2601, 1999.

[41] T. C. L. Wee, "Novel quantum well intermixing technique using Ar-plasma exposure," M.Eng. thesis, Nanyang Technological Univ., School of Electrical and Electronic Engineering, Singapore, 2000.

[42] M. A. Liberman and A. J. Lichtenberg, *Principles of Plasma Discharges and Materials Processing*. New York: Wiley, 1994.

H. S. Djie (S'03) received the B.Eng. degree in electrical engineering from Pelita Harapan University, Indonesia, in 1999 under the Lippo Group scholarship. He is currently working toward the Ph.D. degree at Nanyang Technological University, Singapore.

His current research interests are the physics of low-dimensional quantum structures, the plasma-based semiconductor process, quantum-well intermixing, single-mode/tunable laser diode design and fabrication, and photonics integrated circuits.

T. Mei (M'00) was born in Jiangsu, China, on November 8, 1965. He received the B.S. and M.S. degrees in optical engineering from Zhejiang University, Hangzhou, China, in 1988 and 1991, respectively, and the Ph.D. degree in electrical engineering from the National University of Singapore, Singapore, in 2000.

He is currently an Assistant Professor of Electrical and Electronic Engineering at Nanyang Technological University, Singapore. His research areas have included optoelectronics, compound semiconductor quantum devices, silicon MEMS devices, and infrared imaging technology. His current research activities involve quantum-well intermixing, photonic integration, QWIPs based on intersubband transition, and infrared sensors using silicon micro-machining technology.

J. Arokiaraj was born in Chennai, India, on May 16, 1967. He received the B.Sc. and M.Sc. degrees in physics from Loyola College under Madras University, Chennai, Tamil Nadu, India, in 1998 and 1990, respectively, and the M.Phil. degree and the Ph.D. degree in science and humanities from Anna University, Chennai, India, in 1997.

He is currently a Research Fellow in the School of Electrical and Electronic Engineering, Nanyang Technological University, Singapore. His research areas involve the growth of bulk crystal growth of III-V compounds and thin-film epitaxial growth by metal–organic chemicap vapor deposition. He also specializes in materials characterization by photoluminescence. His major interest is in wafer bonding of III-V materials on Si substrates. His current research is on quantum-well intermixing for bandgap tuning.

C. Sookdhis received the B.S. degree in physics from Mahidol University, Thailand, in 1999 and the M.S. degree in applied optics from Imperial College of Science, Technology, and Medicine, London, U.K., in 2000.

He is currently a research student in the Photonics Group, School of Electrical and Electronic Engineering, Nanyang Technological University, Singapore. His research interests are tunable semiconductor lasers and waveguide devices.

S. F. Yu (M'03-SM'03) received the Degree of Bachelor of Engineering (first class Honours) in electronic engineering from London University, University College, London, U.K., in 1990 and the Ph.D. degree in optoelectronics engineering from Cambridge University, Robinson College, Cambridge, U.K., in 1993.

He joined the Department of Electronic Engineering, Sha Tin Technical Institute, Hong Kong, as a part-time Lecturer in 1993. In 1994, he joined the Department of Electrical & Electronics Engineering, The University of Hong Kong, where he was a Lecturer. Since 1996, he has been an Assistant Professor in the same department. In 2000, he worked at Agere System (formerly Optoelectronic Center, Lucent Technologies Inc., in Breinigsville, PA, as a Member of Technical Staff. In 2001, he joined the School of Electrical and Electronic Engineering, Nanyang Technological University, Singapore.

L. K. Ang (S'95–A'99) received the B.S. degree from National Tsing Hua University, Taiwan, R.O.C., in 1994, and the M.S. and Ph.D. degrees from the University of Michigan, Ann Arbor, in 1996 and 1999, respectively.

He was awarded a fellowship to work as a Los Alamos National Laboratory Director Post-Doctoral Fellow in the Applied Physics Division from 1999 to 2001. Since September 2001, he has been an Assistant Professor with the Division of Microelectronics, School of Electrical and Electronic Engineering, Nanyang Technological University, Singapore. His research interests focus on theoretical analysis and simulation of beam and plasma-related systems. He is presently working on analysis of intense beam-nanostructures interaction, vacuum microelectronics and nanoelectronics. He is also interested in the simulation of plasma process for nanostructure thin film deposition for gas sensor application, and plasma-induced quantum-well intermixing for photonic applications. He has authored or coauthored approximately 50 journal and conference papers, including two invited papers and twoinvited talks.

Dr. Ang is a member of the American Physical Society.

X. H. Tang received the B.S. degree from Fudan University, Shanghai, China, in 1982 and the Ph.D. degree from the National University of Singapore in 1998.

He joined in Hewlett-Packard/Agilent Technologies Singapore, Pte., Ltd., in 1996 as a Process Engineer woking on semiconductor LED wafers. In 2000, he joined Nanyang Technological University, Singapore, engaged in research on III-V semiconductor metal–organic chemical vapor deposition epitaxy growth. His research areas are in the epitaxial growth of semiconductor low-dimension structures, their electrical and optical properties, and their applications in optoelectronic devices.